

Large scale structure simulations of inhomogeneous LTB void models

David Alonso¹, Juan García-Bellido^{1,2}, Troels Haugbølle^{3,4,1} and Julián Vicente¹

¹ *Instituto de Física Teórica UAM-CSIC, Universidad Autónoma de Madrid, Cantoblanco, 28049 Madrid, Spain,*

² *Dép. Physique Théorique, Univ. Genève, 24 quai Ernest Ansermet, CH-1211 Genève 4, Switzerland*

³ *Niels Bohr International Academy, Niels Bohr Institute, Blegedamsvej 17, 2100 Copenhagen, Denmark*

⁴ *Department of Physics and Astronomy, University of Aarhus, DK-8000, Aarhus, Denmark*

(Dated: 15 October, 2010)

We perform numerical simulations of large scale structure evolution in an inhomogeneous Lemaitre-Tolman-Bondi (LTB) model of the Universe. We follow the gravitational collapse of a large underdense region (a void) in an otherwise flat matter-dominated Einstein-deSitter model. We observe how the (background) density contrast at the centre of the void grows to be of order one, and show that the density and velocity profiles follow the exact non-linear LTB solution to the full Einstein equations for all but the most extreme voids. This result seems to contradict previous claims that fully relativistic codes are needed to properly handle the non-linear evolution of large scale structures, and that local Newtonian dynamics with an explicit expansion term is not adequate. We also find that the (local) matter density contrast grows with the scale factor in a way analogous to that of an open universe with a value of the matter density $\Omega_M(r)$ corresponding to the appropriate location within the void.

PACS numbers: 98.80.Cq

IFT-UAM/CSIC-10-54

I. INTRODUCTION

Distant supernovae appear dimmer than expected in a purely matter-dominated homogeneous and isotropic FRW universe. The currently favoured explanation of this dimming is the late time acceleration of the universe due to an energy component that acts like a repulsive force. The nature of the so-called Dark Energy responsible for the apparent acceleration is completely unknown. Observations seem to suggest that it is similar to Einstein's cosmological constant, but there is inconclusive evidence [1]. In the meantime, our realization that the universe around us is far from homogeneous, since there are large superclusters and huge voids across our largest galaxy catalogs [2] has triggered the study of alternatives to this mysterious energy. Since the end of the nineties it has been suggested by various groups [3, 4] that an isotropic but inhomogeneous Lemaitre-Tolman-Bondi universe could also induce an apparent dimming of the light of distant supernovae, in this case due to local spatial gradients in the expansion rate and matter density, rather than due to late time acceleration. There is nothing wrong or inconsistent, apart from philosophical prejudices, with the possibility that we live close to the centre of a gigaparsec-sized void. Such a supervoid may indeed have been observed as the CMB cold spot [5] and somewhat smaller voids have been seen in the local galaxy distribution [6, 7]. If a local void had the size and depth of a void responsible for the cold spot, i.e. $r_0 \sim 2$ Gpc and $\Omega_M \sim 0.2$ within a flat Einstein-de Sitter universe, it would be consistent with local observations [8, 9], and could account for the supernovae dimming, together with the observed baryon acoustic oscillations and CMB acoustic peaks, the age of the universe, local rate of expansion, etc. [4, 10–15].

In order to make contact with large scale structure

observations of the matter distribution, large numerical simulations are usually performed, where a very specific initial condition is assumed for the primordial spectrum of inhomogeneities and the evolution is done solving the Newtonian dynamics numerically. In most cases, the matter content is just cold dark matter falling into gravitational potential wells set in by inflation, although some simulations have included also baryons as well as hot dark matter, neutrinos, radiation, and astrophysical feedbacks.

This conceptually simple recipe yields results which are in good agreement with the matter distribution we observe in the sky on large scales, and can be used to constrain our model of the Universe and determine some of the parameters of the Standard Model of Cosmology. However, some have argued (see e. g. [16] and references therein) that the late stages of gravitational collapse, and structure formation in the universe require a fully relativistic numerical description in order to capture specific signatures of the strong non-linear dynamics of general relativity, and make a correct treatment of features even with sizes comparable to the Hubble radius, see also [17–19].

In this paper we have tested the validity of the Newtonian approximation for structure formation in the context of an inhomogeneous model whose fully non-linear dynamics can be solved exactly using the Einstein equations [3, 4]. We start with an Einstein-deSitter model at a high redshift, and we test it under various initial conditions: i) We first include just a large void of fixed size and a small initial amplitude, and we follow the non-linear growth of the void's depth and size; ii) We then add Cold Dark Matter (CDM) with a Gaussian random field distribution based on inflation ($n_s = 1$ and $\sigma_8 = 0.9$), with the weighted matter-baryon transfer function included to account for the Baryon Acoustic Oscillations (with $f_{\text{gas}} = 0.14$ and $\Omega_{\text{tot}} = 1$ consistent with WMAP-7yr),

and follow the growth of both the void and the matter power spectrum. We have confirmed that our numerical simulations follow the exact solution of the LTB background Einstein equations at all scales (radii), except for very extreme cases, where shell crossing occur in models with large scale structure fluctuations (shell crossing does not occur though if we take a pure void). This seem to suggest that the Newtonian approximation for gravitational collapse is perfectly valid, even for gigaparsec-sized voids as empty as $\Omega_M = 0.02$ at the centre at $z = 0$, which corresponds to density contrasts of order 1 with respect to the asymptotic EdS model. We obtain very good matches to both the density and the velocity profile for matter moving in such LTB backgrounds. We also check that the non-linear evolution gives rise to well differentiated Hubble rates along the line of sight and transverse directions, in perfect agreement with the exact relativistic solutions. Moreover, we can follow the evolution of the matter density contrast as a function of the scale factor and find that it evolves as one would expect for an open universe with the value of $\Omega_M(r)$ corresponding to the local position within the void.

II. LEMAÎTRE-TOLMAN-BONDI VOID MODELS

The Lemaître-Tolman-Bondi model describes general spherically symmetric space-times and can be used as a toy model for describing large voids in the universe. The metric is given by

$$ds^2 = -dt^2 + \frac{A'^2(r, t) dr^2}{1 - k(r)} + A^2(r, t) (d\theta^2 + \sin^2 \theta d\phi^2),$$

with a spherically symmetric matter source with negligible pressure, $T^\mu_\nu = -\rho_M(r, t) \delta^\mu_0 \delta^\nu_0$. Since we have different radial and angular scale factors, we also define a transverse and longitudinal Hubble rates as $H_T \equiv \dot{A}/A$, and $H_L \equiv \dot{A}'/A'$, where dots and primes denote ∂_t and ∂_r , respectively. Integrating the Einstein equations for this metric one finds the r -dependent transverse Hubble rate

$$\frac{H_T^2(r, t)}{H_0^2(r)} = \Omega_M(r) \left(\frac{A_0(r)}{A(r, t)} \right)^3 + \Omega_K(r) \left(\frac{A_0(r)}{A(r, t)} \right)^2,$$

where we have fixed the gauge by setting $A_0(r) = r$ and $\Omega_K(r) = 1 - \Omega_M(r)$. For fixed r the above equation is equivalent to the Friedmann equation, and has an exact parametric solution, see Ref. [4].

In general, LTB models are uniquely specified by the two functions $H_0(r)$ and $\Omega_M(r)$, but to test them against data we have to parameterize the functions, to reduce the degrees of freedom to a discrete set of parameters. For simplicity in this paper we will use the constrained GBH model [4] to describe the void profile. First of all, it uses a minimum set of parameters to make a simple void profile, and secondly, we impose that the time to Big Bang

should be constant. We have made this choice, because models with an inhomogeneous Big Bang would contain a mixture of growing and decaying modes, and consequently the void would not disappear at high redshift, making them incompatible with the Standard Big Bang scenario [20]. If we only consider constrained LTB models, then at high redshifts and/or at large distances the central void is reduced to an insignificant perturbation in an otherwise homogeneous universe described by an FRW metric, and physical results for the early universe derived for FRW space-times still hold, even though we are considering an LTB space-time. The second condition gives a relation between $H_0(r)$ and $\Omega_M(r)$, and hence constrain the models to one free function, and a proportionality constant describing the overall expansion rate. Our chosen model is thus given by [4, 10]

$$\begin{aligned} \Omega_M(r) &= 1 + (\Omega_{\text{in}} - 1) \left(\frac{1 - \tanh[(r - r_0)/2\Delta r]}{1 + \tanh[r_0/2\Delta r]} \right) \\ H_0(r) &= H_0 \left[\frac{1}{\Omega_K(r)} - \frac{\Omega_M(r)}{\sqrt{\Omega_K^3(r)}} \sinh^{-1} \sqrt{\frac{\Omega_K(r)}{\Omega_M(r)}} \right] \end{aligned}$$

where we have assumed that space is asymptotically flat, $\Omega(\infty) = 1$. The model has then only four free parameters: The overall expansion rate H_0 , the underdensity at the centre of the void Ω_{in} , the size of the void r_0 , and the transition width of the void profile Δr . For more details on the model see Ref. [4].

III. LINEAR PERTURBATION THEORY

We still do not have a complete linear perturbation theory for LTB models. The main difficulty is that since the background is inhomogeneous we cannot split the perturbations into independent equations for the scalar, vector and tensor modes. In LTB models the equations for these modes appear as coupled partial differential equations [20, 21]. In particular, the scalar modes couple to the tensor shear modes at first order, which act as source for the scalar mode via the background shear. However, in the case that the latter is small, like in the models we have been describing in our previous works [11], we can ignore this source and solve *exactly* the perturbation equation for the scalar mode Φ , which in the absence of anisotropic matter stresses is equal to the curvature mode Ψ . In this approximation the equation becomes

$$\ddot{\Phi}(r, t) + 4H_T(r, t)\dot{\Phi}(r, t) - \frac{2k(r)}{A^2(r, t)}\Phi(r, t) = 0, \quad (1)$$

with the exact solution

$$\Phi(r, t) = \Phi_0(r, 0) {}_2F_1 \left[1, 2, \frac{7}{2}, \left(1 - \Omega_M^{-1}(r) \right) \frac{A(r, t)}{r} \right]. \quad (2)$$

We note that, strictly speaking, this solution is only exact when ignoring the tensor coupling, and considering

angular transverse modes, but turns out to be a very good approximation. In that same approximation (negligible background shear), the density contrast of matter is proportional to the scalar metric perturbation,

$$\delta(r, t) = \delta_0(r) \frac{A(r, t)}{r} \frac{\Phi(r, t)}{\Phi_0(r, 0)}, \quad (3)$$

where $\delta_0(r)$, up to a normalization factor, can be determined under the assumption that the small scale matter perturbations in the early universe decouple from the void, giving $\delta_0(r) \propto r/A(r, t_{\text{early}})$. It is this function which we will try to compare with the simulations described in the next section.

IV. NUMERICAL SIMULATIONS

To test the validity of N-Body codes in describing gigaparsec sized voids, and to follow the evolution and formation of structure in such models, we have modified the 2LPT initial condition generator [22] to set up an N-Body simulation of a void for the **Gadget2** code [23] where the displacements and velocities of the particles are found using second order Lagrangian perturbation theory [22]. Starting with a standard transfer function for the total matter content in a flat Einstein-deSitter model we construct initial conditions for the gravitational potential in k -space $\Phi_{\mathbf{k}}^i$. Then we find the gravitational potential of a void $\Phi_{\mathbf{k}}^v$ using the analytical solution, by interpolating the density out on the particle grid, and then Fourier transforming it. Now that the total potential $\Phi_{\mathbf{k}} = \Phi_{\mathbf{k}}^i + \Phi_{\mathbf{k}}^v$ is known, the 2LPT code proceeds unchanged from the original version. Once the initial conditions have been set up we use the public domain version of the **Gadget2** code in pure tree-mode to run the simulation (see table I for an overview of the simulations) [28].

It is not evident that N-body simulations can be used to describe large scale LTB models, and therefore a significant effort has gone into validating that indeed we reproduce the expected theoretical behaviour. To test the code we have used different starting redshifts ($z_{\text{start}}=24, 49, 99$, and 199) to check explicitly that the code is started at high enough redshifts, such that the displacements of the particles are much smaller than the inter-particle distance, and that the void can be treated as a linear perturbation, which at first order does not interact with the small scale fluctuations from the power spectrum. We have used different resolutions (simulations $\mathcal{S}24$ and \mathcal{H} – see table I) to test that the cosmological large scale structure is adequately resolved, we have tested that the void does not interact too much with mirror images of itself by changing the physical box size from $L=2400$ to $L=3600$ $\text{Mpc } h^{-1}$ (simulations $\mathcal{S}49$ and \mathcal{L}), and we have checked that to first order the small scale fluctuations do not back react significantly on the void, by running with and without matter perturbations (simulations $\mathcal{S}49$ and \mathcal{V}). Apart from the numerical tests, we have simulated a representative set of realistic void models varying the tran-

Name	z_{start}	Ω_{in}	$\Delta r/r_0$	#particles	Comments
\mathcal{H}	24	0.25	0.3	960^3	High res sim
\mathcal{V}	49	0.25	0.3	512^3	Void alone
$\mathcal{S}24$	24	0.25	0.3	512^3	Void + matter
$\mathcal{S}49$	49	0.25	0.3	512^3	Void + matter
$\mathcal{S}99$	99	0.25	0.3	512^3	Void + matter
$\mathcal{S}\Omega 125$	49	0.125	0.3	512^3	Void + matter
$\mathcal{S}\Omega 063$	49	0.0625	0.3	512^3	Void + matter
$\mathcal{S}\Omega 021$	199	0.0208	0.3	512^3	Void + matter
$\mathcal{S}\Delta 01$	49	0.125	0.1	512^3	Void + matter
$\mathcal{S}\Delta 05$	49	0.125	0.5	512^3	Void + matter
\mathcal{L}	49	0.25	0.3	768^3	$L=3600 \text{ Mpc } h^{-1}$

TABLE I: Overview of the simulations. All have been performed with a void of radius $r_0=1100 \text{ Mpc} = 473 \text{ Mpc } h^{-1}$, and with an asymptotic Hubble parameter of $h_\infty = 0.43$. The standard box size is $L=2400 \text{ Mpc } h^{-1}$, and the particle mass is $M_{\text{part}} = 2.8 \times 10^{13} M_\odot h^{-1}$ ($M_{\text{part}} = 4.3 \times 10^{12} M_\odot h^{-1}$ for \mathcal{H}). Everywhere we have used a smoothing length of $56 \text{ kpc } h^{-1}$ (except for \mathcal{H} , where it has been appropriately rescaled).

sition length $\Delta r/r_0$ and central underdensity Ω_{in} (see table I). The majority of the simulations use a GBH model with $\Omega_{\text{in}} = 0.25$, and $\Delta r/r_0 = 0.3$, but we have also run other simulations with $\Omega_{\text{in}} = 0.125$, $\Omega_{\text{in}} = 0.0625$, $\Omega_{\text{in}} = 0.0208$, and $\Delta r/r_0 = 0.1$ and $\Delta r/r_0 = 0.5$.

V. ANALYSIS AND RESULTS

The results in this paper show the concordance between the simulations and the theoretical predictions. In order to check this we use the highest resolution simulation \mathcal{H} as our reference model and the other simulations to test the limits of the validity of N-Body simulations for describing LTB models. We have subjected our simulation to three different tests, confronting the density profile, the Hubble parameter profile (H_T and H_L) and the density contrast evolution with the corresponding theoretical predictions.

A. Distances and redshifts in LTB models.

Gadget2 is designed to perform simulations of FRW universes, and one needs to associate the comoving radial coordinates in both models. Since we have analyzed the data from **Gadget2** snapshots, that is, positions and velocities of particles are “measured” at constant cosmic time, and all our observables are quantities calculated in thin spherical shells, this identification must be done through the proper radial distance, calculated in both cases as

$$d_p(r, t) = a(t) r_{\text{FRW}} = \int_0^{r_{\text{LTB}}} \frac{A'(r, t)}{\sqrt{1 - k(r)}} dr. \quad (4)$$

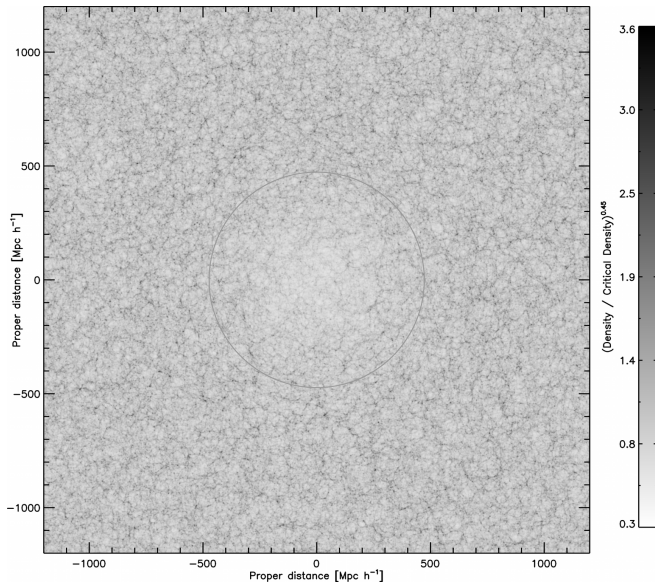


FIG. 1: The projected matter distribution at $z = 0$ averaged over a 175 Mpc slice centered on the void of the 960³ simulation. Notice how near the centre of the void, not only the density is lower, but also there is significantly less structure than outside the void. The characteristic void size $r_0 = 473 \text{ Mpc } h^{-1}$ is indicated by the thin circle.

When the curvature factor $(1 - k(r))^{-1/2}$ is roughly 1, which is the case in the models under study, one can approximate

$$d_p(r, t) = a(t) r_{\text{FRW}} \simeq A(r_{\text{LTB}}, t) \quad (5)$$

for most redshifts. Similarly, when interpreting the results, it is important to remember that while the proper cosmological time in the two metrics can readily be identified, the redshift at equal times are different, i.e. for $t_{\text{FRW}} = t_{\text{LTB}}$ the z_{FRW} and z_{LTB} are different. It is important to emphasize that since we are considering a constrained-GBH LTB model, the time to Big Bang is homogenous and thus all times at each radial distance are the same, so each particle in the simulation has a time given by the code: $t_{\text{FRW}} = t_{\text{LTB}}$.

B. Density profile

We first compare the theoretical density profile of a GBH universe having the desired parameters with the corresponding profile obtained from the simulation. The density field is calculated by interpolating each particle in the box to a grid using a 2nd order triangular-shaped-cloud (TSC) technique [24] (see fig. 1); then the simulation box is divided into different spherical bins, and we calculate the average density in each of them thus obtaining the density as a function of the proper distance d_p (see eq. 4). Due to the presence of non-linear inhomogeneities, the error in the determination of the density

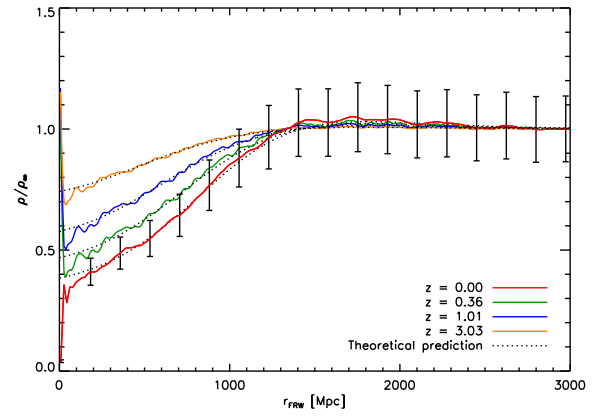


FIG. 2: Comparison of the density profile of the \mathcal{H} simulation at different redshifts with the theoretical curves, as a function of comoving distance $r_{\text{FRW}} = (1 + z)d_p$ in Mpc.

profile cannot be directly obtained as the r.m.s. in each bin, and the error bars displayed in the figures have been calculated as the r.m.s. in the analogous \mathcal{V} simulation without CDM perturbations. The reference simulation \mathcal{H} shows an excellent agreement between theory and simulation (see fig. 2), except near the centre of the void, where the particle distribution is undersampled and shot noise dominated.

In fig. 3 we show the density profile for an extended set of models. For most models the simulations are in excellent concordance with the theory, though for two extremal cases, namely the emptiest void $\mathcal{S}\Omega 021$, and the void with the steepest transition $\mathcal{S}\Omega\Delta 01$ we find significant deviations. For $\mathcal{S}\Omega\Delta 01$ the discrepancy is not severe, and only present in the density profile. We speculate that this could be due to under resolution of the transition length or possibly due to the small-scale perturbations interacting with the large scale void, given that the transition length is only $\Delta r = 47.3 \text{ Mpc } h^{-1}$.

C. Rates of expansion

The radial velocity profile can be used to compare against the theoretical predictions for H_T and H_L . The rate of change in the proper distance \dot{d}_p/d_p computed in the rest-frame of the matter should match each other in the FRW and LTB metric, if the simulations are a valid description of the LTB model. In the LTB metric matter is at rest, and keeps the same comoving coordinate, while in the FRW metric there are systematic radial motion, and We have that

$$\frac{d}{dt} d_p^{\text{FRW}} = \frac{d}{dt} [a r_{\text{matter}}] = d_p [\langle v_r \rangle / r + H_\infty], \quad (6)$$

which can be directly compared to the theoretical LTB result calculated taking the derivative of the r.h.s. of

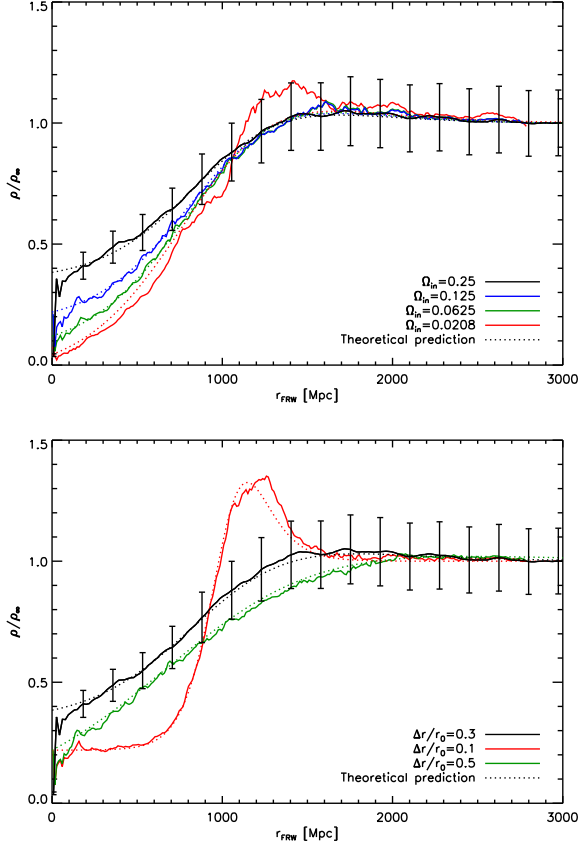


FIG. 3: Density profiles for different values of Ω_{in} (top panel) and $\Delta r/r_0$ (lower panel) in comparison with the corresponding theoretical profiles. All curves are plotted at redshift $z = 0$.

eq. (4). $\langle v_r \rangle$ is calculated as the average radial velocity v_r of the particles sampled in spherical bins. In the upper panel of fig. 4 we see how the theoretical radial velocities (calculated from $a^{-1}[\dot{d}_p - H_\infty d_p]$) match the data from \mathcal{H} . We have found that \dot{d}_p/d_p approximate H_T very well (see eq. 5), possibly because the denominator in eq. (4), $(1 - k(r))^{-1/2}$, being time independent, cancel in the ratio \dot{d}_p/d_p . Using this approximation in the lower panel of fig. 4 we compare a range of models to theory. Again, the difference with the theoretical graph found near $d_p = 0$ is understandable, we are shot noise dominated, and furthermore the matter perturbations displace the centre of the void slightly, while at the same time we have a formal singularity at $r = 0$ when calculating $\langle v_r \rangle/r$. From H_T we can extract H_L straightforwardly as :

$$H_L = \frac{\dot{A}'}{A'} = H_T + \frac{A}{A'} H'_T, \quad (7)$$

which is just $H_L = H_T + r H'_T$ at $z = 0$, using $A_0(r) = r$. We stress though, that at $z = 0$ this is a derived parameter, and not independent of $H_T(d_p)$. We find that all but the emptiest model $\mathcal{S}021$ match well the theoret-

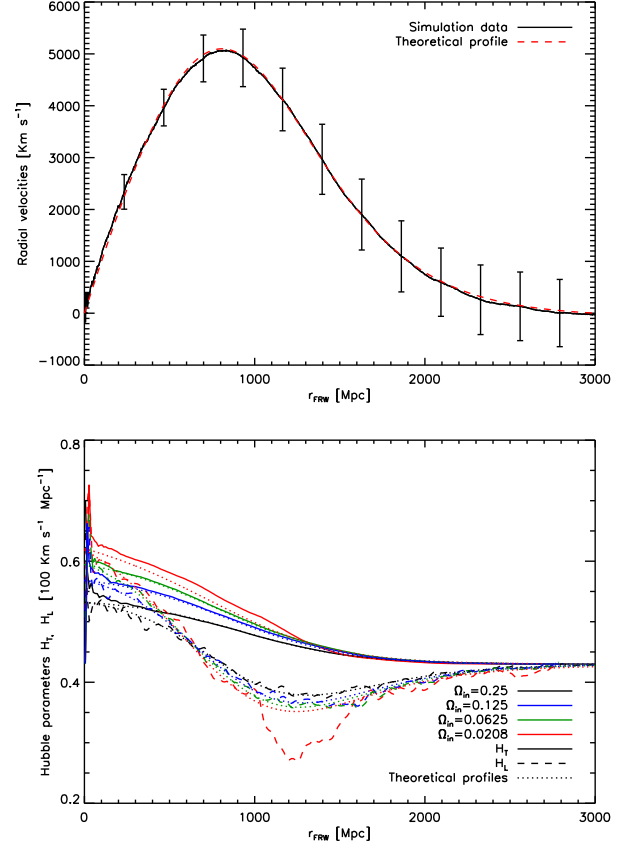


FIG. 4: The velocity profile for the simulation \mathcal{H} (top panel) and the H_T and H_L profiles for different values of Ω_{in} (lower panel). In both cases, the theoretical profiles are shown with dotted lines. All curves are plotted at redshift $z = 0$.

ical predictions. For $\mathcal{S}021$ the velocity is consistently higher (and the density lower) inside the void compared to theoretical predictions, and a density spike is building up near the edge of the void. This could be due to the very lower density, but it may also be a consequence of the very high starting redshift ($z_{\text{start}} = 199$), that was necessary to keep the perturbations linear and the particle displacements acceptable in the initial condition.

D. Density contrast

Another interesting observable to study is the evolution of the density contrast as a function of redshift, $\delta(z) = (\rho(z) - \bar{\rho})/\bar{\rho}$. Being (random) fluctuations, we calculate it by finding the r.m.s. of $\delta(z)$ in spherical bins as a function of proper distance. The errors in the determination of δ were calculated as the standard deviation of the values of δ calculated in the 8 octants of each spherical bin. The results for the simulation $\mathcal{S}49$ can be seen in fig. 5, where we compare the density contrast, calculated at a fixed comoving distance $r_{\text{FRW}} = (1 + z)d_p$,

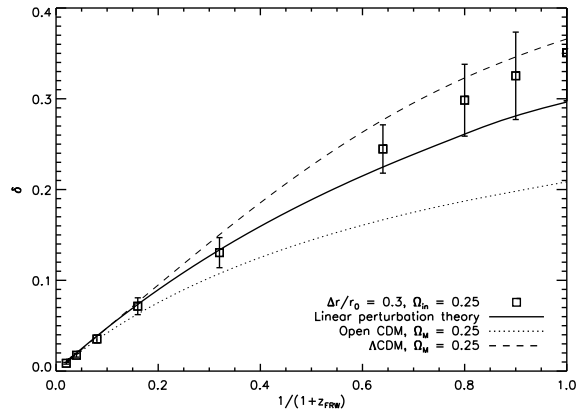


FIG. 5: Density contrast evolution inside the void at comoving distance $r_{\text{FRW}} = (1+z)d_p = 280$ Mpc, for $\mathcal{S}49$, in comparison with the theoretical prediction from perturbation theory (full line). We also compare the LTB growth of density perturbations with that of Open CDM (dotted line) and Λ CDM (dashed line). The theoretical curves were normalized to have the same slope asymptotically in the past, as $a_{\text{FRW}} \rightarrow 0$. Note that, even though the horizontal axis reads $1/(1+z_{\text{FRW}})$, this z_{FRW} only determines the cosmic time t , since the density contrast was calculated at a fixed comoving distance, and not in the lightcone.

as a function of time (expressed in terms of redshift), with the predicted one within the simplified linear perturbation theory in LTB described by eq. (3). We also include, for comparison, the density contrast growth for an open universe, with $\Omega_M = 0.25$, and a Λ CDM, with $\Omega_M = 0.25$ and $\Omega_\Lambda = 0.75$. It is interesting to note that the data agree well, within error bars, with both the theoretical prediction in the LTB model and in the concordance Λ CDM, while they differ significantly from an open universe with the same matter density.

In order to better understand these differences, we have also studied the evolution of the density contrast at several distances from the center of the void. The results are shown in fig. 6. Two clearly different zones can be distinguished: while the growth is proportional to $(1+z)^{-1}$ for large comoving distance, i.e. $\Omega \sim 1$ outside the void and $a_{\text{FRW}} = (1+z)^{-1}$, the growth is significantly slower (as would occur in an open FRW universe), for small distances.

VI. CONCLUSIONS

We have studied for the first time the non-linear evolution of structure formation in large-void LTB models within an asymptotic Einstein-deSitter (EdS) universe. By initiating large N-body simulations at high redshifts, we have been able to follow the non-linear gravitational collapse of matter structures in the presence of an underdense void that starts with a density contrast of or-

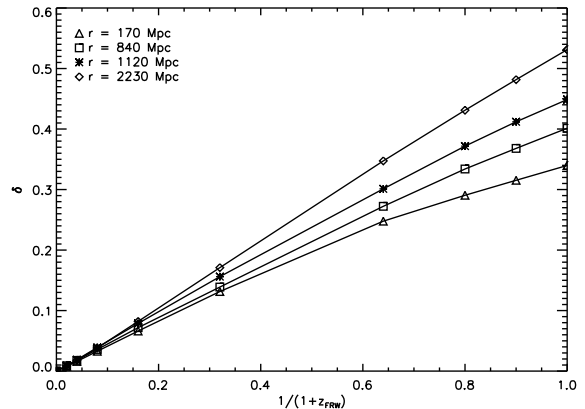


FIG. 6: Density contrast evolution at different fixed comoving distances for $\mathcal{S}49$ simulation, as a function of the FRW scale factor, like in Fig. 5. It is easy to distinguish between the contrast growth in a background with $\Omega \sim 1$ at large distances and with a lower Ω near the void center.

der $\delta_m \sim 10^{-3}$ at photon decoupling (where the matter perturbations have $\delta_m \sim 10^{-5}$). We find that using a standard N-body code, the nonlinear growth of the void underdensity follows the exact analytical solution of the Einstein equations, even for very deep voids with $\Omega_M = 0.06$ at the center, and thus with density contrasts of order one with respect to the asymptotic EdS universe. Moreover, the transverse and longitudinal rates of expansion agree with the theoretical expectations, giving us confidence that the simulations are tracing the full nonlinear gravitational collapse in this non-perturbative LTB background. This is furthermore evidence that N-body codes give a credible and precise description of the standard Λ CDM model, where the voids are of much lesser size, and no general relativistic corrections are needed to describe the large scale evolution.

We have also studied the evolution of the matter density contrast in such a non-trivial background, and found an analytical solution to the approximate equations for the growth of perturbations in the limit of negligible background shear, and shown that the numerical and analytical results are in good agreement. Moreover, the comparison with OCDM and Λ CDM shows that the density contrast growth for our LTB models is very close within errors to that of the concordance Λ CDM models suggested by WMAP-7yr [1].

From our non-linear LTB N-body simulations we can extract predictions for observations of large scale structure, via the two-point angular correlation function, the angular power spectra, the growth of structure, and the density contrast. Our models therefore give the possibility of using both current and future observations of the large scale structure (such as DES [25], EUCLID [26]

and PAU [27]), to constrain LTB models that already provides a viable fit to current observations of the geometry of the Universe.

Acknowledgements

We thank the anonymous referee for very helpful comments on the manuscript. TH acknowledges support from the Danish Natural Science Research Council. JGB thanks the Institute de Physique Théorique

de l'Université de Genève for their generous hospitality during his sabbatical in Geneva. DAM acknowledges support from a JAE-Predoc contract. We also thank the Benasque Center for Science Pedro Pascual, where this work was partially developed. This work is supported by the Spanish MICINN under Project No. AYA2009-13936-C06-06, the CAM project “HEP-HACOS” Ref. S2009/ESP-1473, and by the EU FP6 Marie Curie Research and Training Network “Universe Net” Ref. MRTN-CT-2006-035863. Computer time was provided by the Danish Center for Scientific Computing.

-
- [1] E. Komatsu *et al.*, arXiv:1001.4538 [astro-ph.CO].
 - [2] J. R. I. Gott *et al.*, *Astrophys. J.* **624**, 463 (2005), arXiv:astro-ph/0310571.
 - [3] N. Mustapha, C. Hellaby & G. F. R. Ellis, *Mon. Not. Roy. Astron. Soc.* **292**, 817 (1997); M.-N. Celerier, *Astron. Astrophys.* **353**, 63 (2000); K. Tomita, *Mon. Not. Roy. Astron. Soc.* **326**, 287 (2001); J. W. Moffat, *JCAP* **0510**, 012 (2005); H. Alnes, M. Amarzguioui & O. Gron, *Phys. Rev. D* **73**, 083519 (2006); D. Garfinkle, *Class. Quant. Grav.* **23**, 4811 (2006); K. Enqvist & T. Mattsson, *JCAP* **0702**, 019 (2007); K. Enqvist, *Gen. Rel. Grav.* **40**, 451 (2008); T. Mattsson, arXiv:0711.4264 [astro-ph]; D. L. Wiltshire, arXiv:0712.3984 [astro-ph].
 - [4] J. Garcia-Bellido and T. Haugboelle, *JCAP* **0804**, 003 (2008), arXiv:0802.1523 [astro-ph].
 - [5] M. Cruz *et al.*, *Mon. Not. Roy. Astron. Soc.* **369** 57 (2006); *Astrophys. J.* **655** 11 (2007); *Mon. Not. Roy. Astron. Soc.* **390** 913 (2008).
 - [6] W. J. Frith, G. S. Busswell, R. Fong, N. Metcalfe & T. Shanks, *Mon. Not. Roy. Astron. Soc.* **345** 1049 (2003)
 - [7] B. R. Granett, M. C. Neyrinck & I. Szapudi, *Astrophys. J. Lett.* **683**, L99 (2008).
 - [8] R. B. Tully, arXiv:0708.0864 [astro-ph].
 - [9] A. Kashlinsky, F. Atrio-Barandela, D. Kocevski and H. Ebeling, *Astrophys. J. Lett.* **686**, L49 (2008).
 - [10] J. Garcia-Bellido and T. Haugboelle, *JCAP* **0809**, 016 (2008), arXiv:0807.1326 [astro-ph];
 - [11] J. Garcia-Bellido and T. Haugboelle, *JCAP* **0909**, 028 (2009), arXiv:0810.4939 [astro-ph].
 - [12] T. Biswas, A. Notari and W. Valkenburg, arXiv:1007.3065 [astro-ph.CO].
 - [13] C. Clarkson and M. Regis, arXiv:1007.3443 [astro-ph.CO].
 - [14] A. Moss, J. P. Zibin and D. Scott, arXiv:1007.3725 [astro-ph.CO].
 - [15] C. M. Yoo, K. i. Nakao and M. Sasaki, *JCAP* **1007**, 012 (2010), arXiv:1005.0048 [astro-ph.CO]; arXiv:1008.0469 [astro-ph.CO].
 - [16] Räsänen, S., *Phys. Rev. D* **81**, 103512 (2010).
 - [17] J. Hwang and H. Noh, *Gen. Rel. Grav.* **38**, 703 (2006); *Mon. Not. Roy. Astron. Soc.* **367**, 1515 (2006).
 - [18] M. N. Bremer, J. Silk, L. J. M. Davies and M. D. Lehnert, arXiv:1004.1178 [astro-ph.CO].
 - [19] M. Mattsson and T. Mattsson, *JCAP* **1010**, 021 (2010), arXiv:1007.2939 [astro-ph.CO].
 - [20] J. P. Zibin, *Phys. Rev. D* **78**, 043504 (2008).
 - [21] C. Clarkson, T. Clifton and S. February, *JCAP* **0906**, 025 (2009), arXiv:0903.5040 [astro-ph.CO].
 - [22] M. Crocce, S. Pueblas & R. Scoccimarro, *Mon. Not. Roy. Astron. Soc.* **373** 369 (2006).
 - [23] V. Springel, N. Yoshida & Simon D. M. White, *New Astron.* **6**, 79, (2001); V. Springel, *Mon. Not. Roy. Astron. Soc.* **364**, 1105 (2005).
 - [24] R.W. Hockney & J.W. Eastwood, “Computer Simulations Using Particles”, Eds. Taylor & Francis (1989).
 - [25] <http://www.darkenergysurvey.org>.
 - [26] <http://sci.esa.int/euclid/>
 - [27] N. Benitez *et al.*, *Astrophys. J.* **691**, 241 (2008), arXiv:0807.0535 [astro-ph.CO]; R. Casas *et al.*, “The PAU Camera,” *Proc. SPIE Int. Soc. Opt. Eng.* **7735**, 773536 (2010).
 - [28] Running Gadget in PM-mode, gives an unphysical imprint both at the edge and at the center of the void, possibly due to the spherical symmetry of the problem.